

# PEG-coated gold nanorod monoclonal antibody conjugates in preclinical research with optoacoustic tomography, photothermal therapy and sensing

Anton V. Liopo, André Conjusteau and Alexander A. Oraevsky  
TomoWave Laboratories Inc., 6550 Mapleridge St., Suite 124, Houston, TX 77081

[www.tomowave.com](http://www.tomowave.com)

## ABSTRACT

Gold nanorods (GNR) with a peak absorption wavelength of 760 nm were prepared using a seed-mediated method. A novel protocol has been developed to replace hexadecyltrimethylammonium bromide (CTAB) on the surface of GNR with 16-mercaptohexadecanoic acid (MHDA) and methoxy-poly(ethylene glycol)-thiol (PEG), and the monoclonal antibodies: HER2 or CD33. The physical chemistry property of the conjugates was monitored through optical and zeta-potential measurements to confirm surface chemistry. The plasmon resonance is kept in the near infrared area, and changes from strong positive charge for GNR-CTAB to slightly negative for GNR-PEG-mAb conjugates are observed. The conjugates were investigated for different cells lines: breast cancer cells and human leukemia lines *in vivo* applications. These results demonstrate successful tumor accumulation of our modified PEG-MHDA conjugates of GNR for HER2/neu in both overexpressed breast tumors in nude mice, and for thermolysis of human leukemia cells *in vitro*. The conjugates are non-toxic and can be used in pre-clinical applications, as well as molecular and optoacoustic imaging, and quantitative sensing of biological substrates.

Key words: gold nanorods conjugation, optoacoustic imaging, cell particle targeting, mice, nanothermolysis and nanosensing

## INTRODUCTION

Gold nanoparticles (NPs) have attracted significant interest as a novel platform for nanobiotechnology and biomedicine because of convenient surface bioconjugation with molecular probes and remarkable optical properties related with the localized plasmon resonance<sup>1-3</sup>. Gold nanoparticles of various shapes have promising biomedical applications in the fields of drug delivery, biomedical imaging, and chemical sensing<sup>4-6</sup>. One type of gold nanoparticle with a strong tunable plasmon resonance in the near-infrared spectral range is the gold nanorod (GNR)<sup>2,7</sup>. After administration into the animal, GNRs get distributed inside the body according to their modified affinity resulting in the enhancement of optical contrast of the targeted tissues<sup>8</sup>. GNRs were also used as optoacoustic (OA) contrast agents for quantitative flow analysis in biological tissues<sup>9</sup> and to investigate the kinetics of drug delivery compounds<sup>8,10</sup>. GNR stabilized with CTAB show strong cytotoxicity and usually require PEG-modification by adding PEG-SH in the CTAB solution<sup>11</sup>. Reasons for PEGylation (i.e. the covalent attachment of PEG) of surfaces nanoparticles are numerous and include shielding of antigenic and immunogenic epitopes, shielding receptor-mediated uptake by the reticuloendothelial system, and preventing recognition and degradation by proteolytic enzymes for biopolymers<sup>10,12-14</sup>. GNR have high optoacoustic contrast, and can be conjugated with specific ligands, such as antibodies, to produce the targeted contrast agents<sup>2</sup>. Recently, we demonstrated that gold nanorods constituted a new nanoparticulate optoacoustic contrast agent<sup>15-17</sup>. GNR can absorb light about one thousand times more strongly than an equivalent volume of an organic dye<sup>2,15</sup>. Demonstrations of photothermal cancer therapy using gold nanorods as a photothermal converter have also been reported by several groups. Targeting gold nanorods to a specific site is both a critical aspect of bioimaging using gold nanorods as a contrast agent, and for achieving efficient photothermal therapy without side effects especially after intravenous injection<sup>13,16,18</sup>. The standard for conjugating gold nanoparticles to antibodies using covalent bonding was published by

several research groups<sup>4,6,19-21</sup>. However, the conjugation processes are in need of improvement. Most protocols are hard to adapt to large-scale manufacturing of highly concentrated conjugates with strong affinity toward factors such as biochemical and physiological conditions of the cells and organs of the body<sup>22</sup>. In these studies, we adopted a published methodology of GNR fabrication<sup>7,23,24</sup> to get high yields of narrow band GNR with an optical absorption centered at 760 nm. The manufactured nanorods were pegylated and conjugated with monoclonal antibody (mAb) to become non-toxic in animals as biocompatible OA contrast agents. We characterized the conjugation efficiency of the GNRs mAb by comparing the efficiency of antibody binding of the GNRs before and after pegylation. We demonstrated new order of PEG-coated gold nanorods monoclonal antibody conjugates in preclinical research with optoacoustic tomography, photothermal therapy and sensing

## MATERIALS AND METHODS

### Fabrication of GNR conjugates

Presented below are the details of our GNR fabrication protocol adapted from previously reported methodology<sup>7,17,25</sup>. The base procedure is tailored to the needs of the specific experiments presented in this paper. It allows high-yield fabrication of a narrow size distribution of rods with a 760 nm plasmon resonance. In a typical procedure, 0.250 mL of an aqueous 0.01 M solution of  $\text{HAuCl}_4 \cdot 3\text{H}_2\text{O}$  was added to 7.5 mL of a 0.1 M CTAB solution in a test tube (15 ml glass tube). Then, 0.600 mL of an aqueous 0.01 M ice-cold  $\text{NaBH}_4$  solution was added all at once. This seed solution was used 2-4 hours after its preparation. In the next step of the fabrication, exact proportions of 4.75 mL of 0.10 M CTAB, 0.200 mL of 0.01 M  $\text{HAuCl}_4 \cdot 3\text{H}_2\text{O}$ , and 0.030 mL of 0.01 M  $\text{AgNO}_3$  solutions were added one at a time in the preceding order, then gently mixed by inversion. The solution at this stage appeared bright brown-yellow in color. Then 0.032 mL of 0.10 M ascorbic acid was added. The solution became colorless upon addition and mixing of ascorbic acid. Ten minutes were allowed for the reaction to fully proceed before adding the required quantity of seed solution. The reaction mixture was gently mixed for 10 seconds and left undisturbed for 1-3 hours. After that the solution was left under thermostatic conditions for 24 hours at the temperature of 30° C.

Before covalent binding with polyethylene glycol (PEG), or conjugation with monoclonal antibody, the GNR were centrifuged at low speed (4000 rpm or 1000 g, 10 min) for separation of other aggregates (platelets, stars). The pellet was removed and for the next steps, only the supernatant fraction was used. For pegylation<sup>11,24,25</sup> the GNR solution was centrifuged at 14000 g for 10 minutes. Following the standard method, 0.1 ml of 2 mM potassium carbonate ( $\text{K}_2\text{CO}_3$ ) was added to 1 ml of aqueous GNR solution and 0.1 ml of 0.1 mM mPEG-Thiol-5000 (Laysan Bio Inc., Arab, AL). The resulting mixture was kept on a rocking platform at room temperature overnight. Excess mPEG thiol was removed from solution by two rounds of centrifugation, and final resuspension occurred in PBS (pH 7.4).

An improved protocol for conjugation of GNR has been developed at TomoWave Laboratories. Early developments of this protocol were described before<sup>21,25</sup>. It involves surface modification of the gold nanorods with Nanothink-16 (or 16-Mercaptohexadecanoic acid, MHDA, Sigma), zero-size linkers, monoclonal antibody and finally pegylation. Detailed steps for the activation of the GNR surface, followed by conjugation, are described next. One mL of raw GNR solution (in CTAB) was centrifuged twice in a 1.5 mL Eppendorf tube at 14000 RPM for 10 min and resuspended in one mL of Milli-Q water (MQW) to a concentration of 1 nM. Then, 10  $\mu\text{L}$  of 5 mM MHDA (in ethanol) was added to the GNR solution, and sonicated for 30 minutes at 50°C to prevent aggregation. The solution was centrifuged at 12000 RPM for 10 minutes, the supernatant was removed and the pellet was resuspended in MQW. 10  $\mu\text{L}$  EDC (1-ethyl-3-[3-(dimethylaminopropyl)] carbodiimide hydrochloride (Pierce) and sulfo-NHS (Pierce) were added from stock solution in MES (2-(4-Morpholino) ethane sulfonic acid) buffer at 10 mM and 0.4 mM, respectively. The mixture was sonicated for 30 minutes at room temperature to produce activated GNR (GNR that are capable of binding to the amine side chain of proteins). Commercial mAb CD33 or HER2 (BD Pharmingen) was added in concentration of 25  $\mu\text{g}/\text{mL}$  to 1 mL of 1 nM activated GNR (Liopo 2011). The mixture was sonicated at room temperature (RT) for 1 hour and then left on a rocking platform overnight, or kept an additional hour at RT. Following the removal of excess mAb by centrifugation, 10  $\mu\text{L}$  of PEG-Thiol (1 mM) was added to 1 mL of GNR-CD33 conjugates and the mixture was incubated at room temperature for 12 h. The solution of GNR CD33 PEG conjugate was centrifuged at 12000 g for 10 minutes, the supernatant was removed and the pellet was resuspended in PBS pH 7.4 to a concentration of 1 nM (or optical density around 4.0 as measured by Beckman 530 and Thermo Scientific Evolution 201 Spectrophotometer). We compare three different methods of activation and conjugation of GNR (see Figure 1). The first method is described above and presented as scheme A.

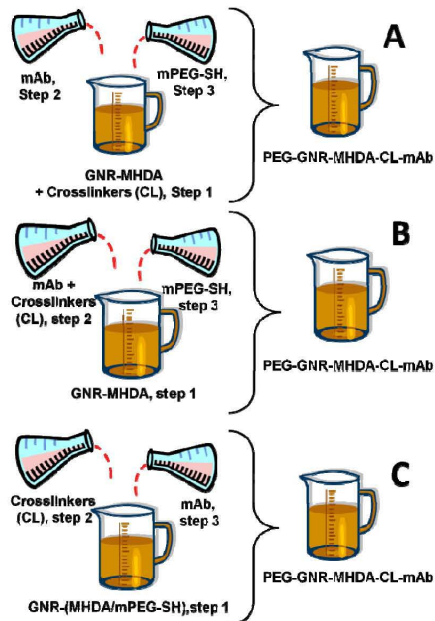


Figure 1. Protocol of GNR conjugates fabrication. See text for detailed conjugation procedures A), B), and C)

The second method of activation, scheme B, has the surface modification performed in another order. Same one mL of synthesized GNR in CTAB was resuspended in one mL of Milli-Q water (MQW). MHDA was added to the GNR-CTAB solution, and the solution was sonicated for 30 minutes at 50°C to prevent aggregation. The solution was centrifuged at 12000 RPM for 10 minutes, the supernatant was removed and the pellet was resuspended in MQW. In parallel, a complex of mAb and crosslinkers was prepared from mAb and solution of EDC/sulfo NHS in MES buffer. The compound was agitated at RT for 30 min. The activated mAb was purified by dialysis or centrifugation with 3000 kDa membrane, and additional washing by salt column (Pierce). The clean complex was added to the GNR-MHDA solution and left overnight (4°C), or 2 h at RT. Following the removal of excess mAb by centrifugation, the GNR-mAb complex was pegylated as shown in method A. The resulting solution of GNR-mAb-PEG conjugate was centrifuged at 12000 g for 10 minutes, the supernatant was removed and the pellet was resuspended in PBS pH 7.4 to a concentration of 1 nM (or optical density around 4.0 as measured by Beckman 530 and Thermo Scientific Evolution 201 Spectrophotometer). The third method of activation of GNR differs also by the order of surface modification steps (scheme C on Fig. 1). Same one mL of synthesized GNR in CTAB was resuspended in one mL of Milli-Q water (MQW). After removal of CTAB, the GNR solution was added to a mixture of MHDA and PEG (in molar ratio 1:5) and the pegylation was performed overnight, as reported in the literature<sup>11,24,25</sup>. The solution was then centrifuged at 12000 RPM for 10 minutes, the supernatant was removed and the pellet was resuspended in MQW. EDC and sulfo-NHS (Pierce) were added from stock solution in MES buffer in 10 mM and 0.4 mM, respectively, and agitated for 30 minutes at RT to pursue the transformation of GNR into PEG-GNR-MHDA. Activation through the carboxy group of MHDA allows binding to the amine side chain of proteins, antibody or peptides. Following the removal of excess EDC/sulfo NHS by centrifugation, commercially available, purified, mAb HER2 or CD33 (BD Pharmingen) was added to the complex. The mixture was agitated at RT for 2 hours, purified by centrifugation, and diluted to working concentration of GNR mAb conjugates. Some experiments were also performed with addition of activated mAb with EDC/sulfo NHS like in scheme B.

### Protein determination and measurements of Zeta-potential

The final step for all methods of conjugation (A,B and C, figure 1) was centrifugation at 12000 g for 10 minutes, the supernatant was removed and the pellet was resuspended in PBS pH 7.4 to the required concentration according to the molar extinction of our GNR ( $3.85 \times 10^9 \text{ M}^{-1}\text{cm}^{-1}$ )<sup>17</sup> and measure of optical density by Beckman 530 or Thermo Scientific Evolution 201 Spectrophotometer). A measure of total and bound protein (mAb CD33) was performed with the Pierce Micro BCA™ Protein Assay Reagent Kit (Pierce). Concentration of CD33 was measured before, and after addition of GNR-activated solution: it is dependent upon either level of Antibody, or incubation time. The determination

was performed through measurement of absorbance at or near 562 nm. It is important to note that the ratio of absorbances at 562 nm (proteins relative to BSA) has a coefficient of variation of only around 10%<sup>17</sup>. The zeta-potential of GNR before and after conjugation was measured with a high performance particle sizer (Malvern Instruments Ltd., Southborough, MA, USA) at 25°C: ten 20-second runs were performed for each sample. Zeta-potential is a measure of both particle stability and adhesion. More negative or positive values of zeta-potential are associated with more stable particle solution, because repulsion between the particles reduces aggregation<sup>26</sup>.

### **Cell Culture, Viability and Tissue Histology**

The human cell lines BT 474 (human breast adenocarcinoma with HER2 receptor overexpression) and human leukemia cells K-562 (chronic leukemia) and HL-60 (acute leukemia), both with CD33 receptor overexpression, were obtained from American Type Culture Collection (ATCC) and were cultured in essential media with 10 % fetal bovine serum<sup>17,25</sup>. Cell viability was determined using a kit for the detection of lactate dehydrogenase activity in medium (LDH, Roche) which was described in our previous works<sup>27</sup>. For assessing viability after nanothermolysis experiments, the cells were slowly centrifuged (500 RPM) and gently resuspended in medium. The toxic effects of GNR were quantified through use of Trypan blue staining. For laser thermotherapy, leukemia cells were pretreated for 45 min with GNR conjugates in concentration of 250 pM (OD 1.0). After centrifugation and removal of supernatant, the cells were resuspended in a small volume of PBS (pH 7.4) and put in a cuvette (25  $\mu$ l), ready for irradiation. After this, the cells were resuspended, and a fraction was stained with Trypan blue in order to count the number of dead and living cells. The remainder was used for LDH determination.

Nude mice were sacrificed 48 h after IV injections of GNRs conjugates. Organs (tumor, spleen and liver) extractions were produced as paraffin-embedded slices for hematoxylin and eosin (HE) and silver (SS) staining<sup>24</sup>. Tissue sections (5  $\mu$ m) were deparaffinized and rehydrated through xylene (3 changes, 5 min each) and graded ethanol solutions from 100 to 50 % (1 min each). After this, samples were rinsed in dH<sub>2</sub>O and placed in a water bath for 10 min with tris-buffered saline with Tween 20 (TBST, Dako, Denmark). Retrieval with Target Retrieval Solution pH 6.1 (TRS, Dako, Denmark) was then performed in a preheated container at 96-99°C for 30-40 min. The slides of liver sections were stained for PEG-GNR optical visualization with a SS Kit (BBI International, UK) according to manufacturer instruction, and HE stained for analysis of possible pathological consequences in liver after PEG-GNR administration.

### **Animal studies of optoacoustic imaging**

We used Athymic Nude-Foxn1<sup>nu</sup> mice (Harlan), 7-9 weeks old, weighing about 25 g. Animal handling, isoflurane anesthesia, and euthanasia were described in detail in our publications<sup>24,28</sup> and each mouse-related procedures were in compliance with our Institutional Animal Care and Use Committee (IACUC) protocol. For optoacoustic imaging, we used mice with tumors that overexpressed HER2/neu receptor in animal models. This model was made through BT474 cells injection ( $2 \times 10^6$ ), subcutaneously in the flank area of nude mice<sup>25</sup>. The tumors had a diameter of 4-6 mm after three-four weeks. The injected solution of GNR conjugates contained from 4 to  $7 \times 10^{12}$  GNR/ml.

In these studies we used a commercial prototype of a three-dimensional optoacoustic tomography system developed for preclinical research at TomoWave Laboratories and introduced in our earlier publications<sup>24,28,29</sup>. The OA mouse imaging system consists of four main components: fiber-optic light delivery, mouse holder with translation and rotation, detector array of 64 transducers, and data acquisition and imaging electronics.

### **NanoLISA prototype.**

We have previously reported on the development of an optoacoustic biosensor intended for the detection of bloodborne microorganisms using immunoaffinity reactions of antibody-coupled gold nanorods as contrast agents specifically targeted to the antigen of interest<sup>30-32</sup>. The sensitivity of Nano-LISA is at least OD= $10^{-6}$  which allows reliable detection of 1 pg/ml (depending on the commercial antibodies that are used). Adequate detection sensitivity, as well as lack of non-specific cross-reaction between antigens favors NanoLISA as a viable technology for biosensor development. Optoacoustic responses generated by the samples are detected using a wide band ultrasonic transducer.

The current transducer design features a 52  $\mu$ m thick polyvinylidene fluoride (PVDF) element attached to an acrylic backing to minimize reflected sound waves and allow efficient damping. On the opposite side, the second electrode is formed by a Mylar sheet that contains a thin metallized layer. This reflective surface completes the circuit and additionally reflects more than 90% of incident light, thus preventing strong pyroelectric response in PVDF film. Based on this design, a prototype sensor was built to measure signals from GNRs adsorbed on a surface of a standard 96-well plate. Samples consisted of 100  $\mu$ l of pegylated GNR solution: each sample is left in the well overnight, as we have observed pegylated nanorods have a tendency to bind strongly to acrylic-type materials. The well is then emptied, and rinsed twice with deionized (DI) water to ensure all loose GNRs are removed from the system, and only a minute layer

of adsorbed GNRs is left on the inner surface of the microwell. After the second rinse, 100  $\mu\text{l}$  of DI water is placed in the well to enhance the signal as the thermal expansion of water is significantly higher than that of acrylic. Through spectrophotometric measurement of optical density of the GNR solution before, and after treatment of the wells, it has been determined that the fraction of GNR that are left in the well is within the measurement error of our instrument. We therefore can put an upper limit on the sticking coefficient of GNRs as 1%. In this case, we determine the upper limit on the GNR number density in the well to be  $3.2 \times 10^6$  GNR/ $\text{mm}^2$ . The actual number of particles contributing to the generation of the optoacoustic response, the population stuck to the bottom of the well, is about  $10^8$  GNRs.

## RESULT AND DISCUSSION

In this study we compare three different methods of activation and conjugation of GNR with mAb (Figure 1). We evaluated the protocol that improves the conjugation process of mAb to GNR and enhances GNR activity toward targeting antibodies. The optimized method of activation of GNR differs by the order of the modification procedure (scheme C). The GNR-CTAB MQW solution is mixed with MHDA and PEG (in molar ratio 1:5), and activated through EDC and sulfo-NHS (Pierce) as the complex PEG-GNR-MHDA. This complex is capable of conjugation through the carboxy group of MHDA for binding with an amine function of proteins, antibody or peptides. The properties of GNR are presented on Figure 2. UV-VIS Spectra of GNR-based contrast agent demonstrates purification of GNR through centrifugation: it was performed to increase the uniformity of the GNR fraction. GNR after PEGylation and GNR after PEGylation and conjugation with mAb HER2 results show the conjugates are stable because their production resulted in a narrow peak around 760nm that matches the biological transparency window<sup>2</sup>.

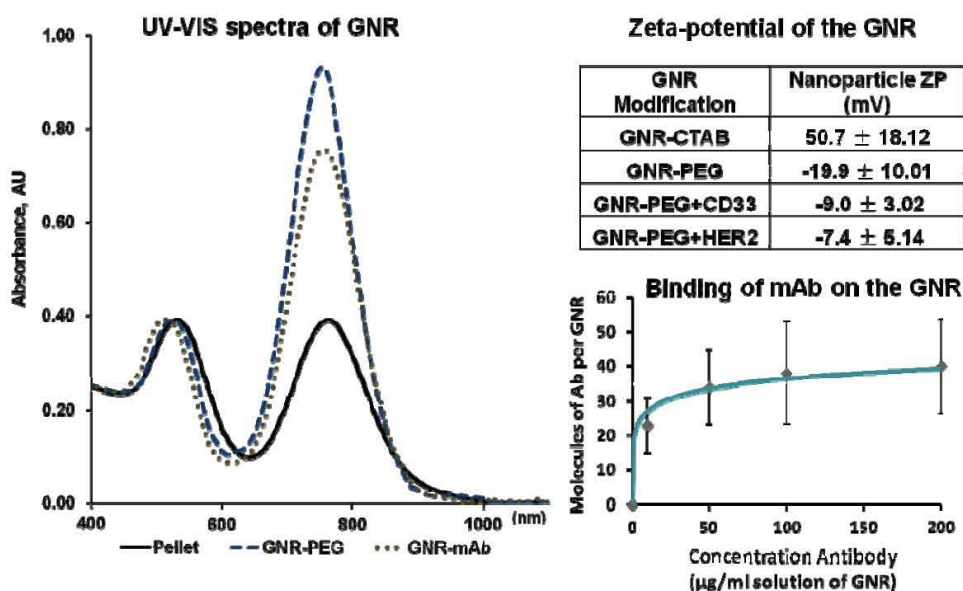


Figure 2. UV-VIS Spectra of GNR-based contrast agent: Pellet after first Centrifugation; GNR after PEGylation (GNR-PEG) and GNR after PEGylation and conjugation with mAb HER2 (GNR-mAb); Zeta-potential of the GNR-CTAB, after GNR PEGylation and their conjugation with CD33 and HER2 mAb; Binding of mAb (CD33) on the surface of activated GNR: effect of mAb concentration

The zeta-potential (Figure 2) of the GNR-CTAB complex was highly positive due to the presence of the positively charged CTAB molecules. The GNR-mAb PEG (both CD33 and HER2) complexes nanoparticles solution showed a zeta-potential which is slightly negative, but significantly different from zero. These results (UV VIS Spectra, and zeta-potential measurements) suggested that this composition is a non-precipitated stable complex. Investigation of binding of mAb (as example anti CD33) on the surface of activated GNR is presented in figure 2 as affected by mAb concentration. Commercial, purified, CD33 (BD Pharmingen) was added in different concentrations from 10 to 200  $\mu\text{g/mL}$  to 1 mL of 1 nM activated GNR<sup>17</sup>. Optimum concentration of CD33 is around 25-50  $\mu\text{g/mL}$  and for HER2 is between 50-100.

Comparison of the different protocols of conjugation with optical microscopy images of breast cancer and human leukemia cells (Figure 3) demonstrated high level of binding for all methods, but the first protocol was extremely difficult; the second needed many steps of purification and is also expensive. The third, scheme C, is reproducible and ready for manufacturing highly concentrated conjugates. High selectivity of GNR-PEG-mAb (HER2) complex is shown in figure 4 for dose dependence effect of attachment of conjugates on cell membrane of breast cancer cells.

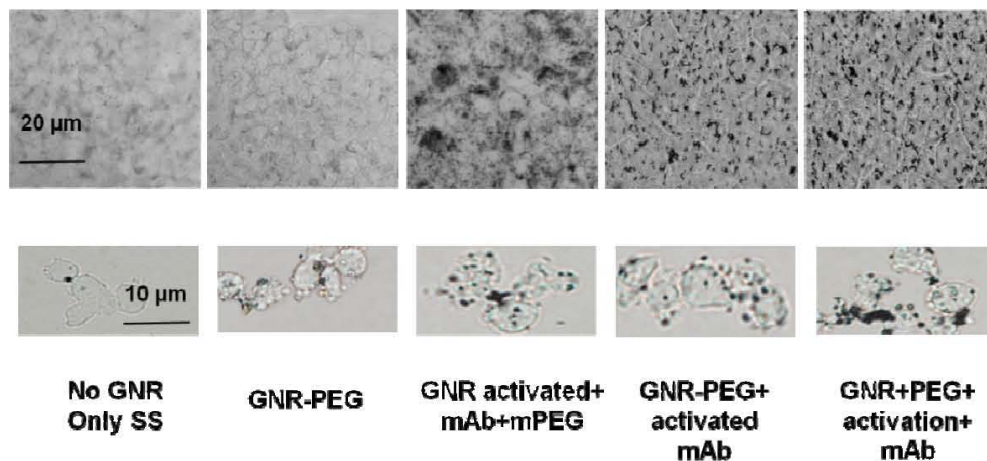


Figure 3. Optical microscopy images of breast cancer BT 474 cells (overexpression of HER2 receptor) and human leukemia K562 cells (overexpression of CD33 receptor) incubated with GNR-PEG, and the three conjugates (A), (B), (C) described in Fig. 1: protocol design (Magnification  $\times 40$ )

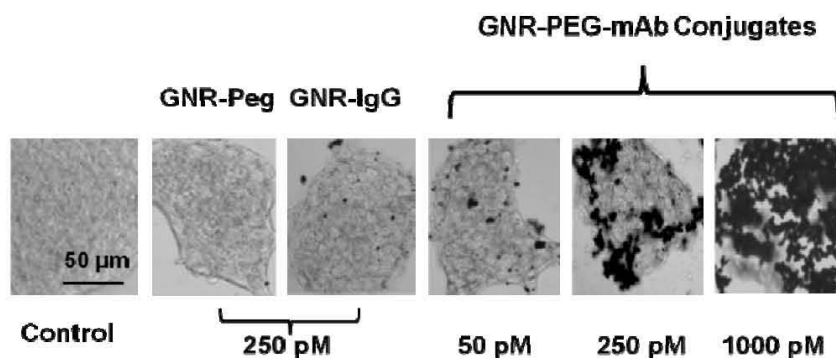


Figure 4. Dose dependence effect of attachment of PEG-GNR-mAb (HER2) conjugates on cell membrane of breast cancer cells BT 474 (incubation time 1 hour, silver staining, magnification  $\times 20$ )

Slices of excised liver, spleen and tissue shown in Figure 5 were taken from another set of mice to track the accumulation of GNR, as well as possible toxicity effects over a span of two days. Silver staining images demonstrate a visible increase of GNR conjugates in tumor, but no specificity in liver after 48 hours following intravenous GNR injection. Interestingly, a visible color change is significant for the liver for both the applications of GNR-PEG and their conjugates. However, the studies with hematoxylin and eosin (HE) staining showed no visible differences between the PBS control and the GNR conjugates slices for spleen and liver. From the HE staining we cannot confirm any morphological changes in mice liver caused by the GNR. Our data is consistent with other reports describing no dangerous physiological changes following the administration of gold nanoparticles or nanorods in vivo<sup>11,14,18,22</sup>. For OA imaging we used intravenous PEG-GNR in dose of 10 mg/kg/BW of mouse. OA results suggested that the enhancement visible on 760 nm images was interpreted as local accumulation of GNRs conjugates. This result is shown in Figure 6. Optoacoustic imaging after GNR-PEG-HER2 injection ( $1.4 \times 10^{12}/0.2$  ml, 24 hour) increases contrast of the tumor area. Another application of conjugated GNR is shown on right side of figure 6: Pulsed-laser nanothermolysis damage to human acute leukemia cells yields 3 fold increase of damage cells targeted with GNR-CD33 measured through release of LDH from cell to medium.

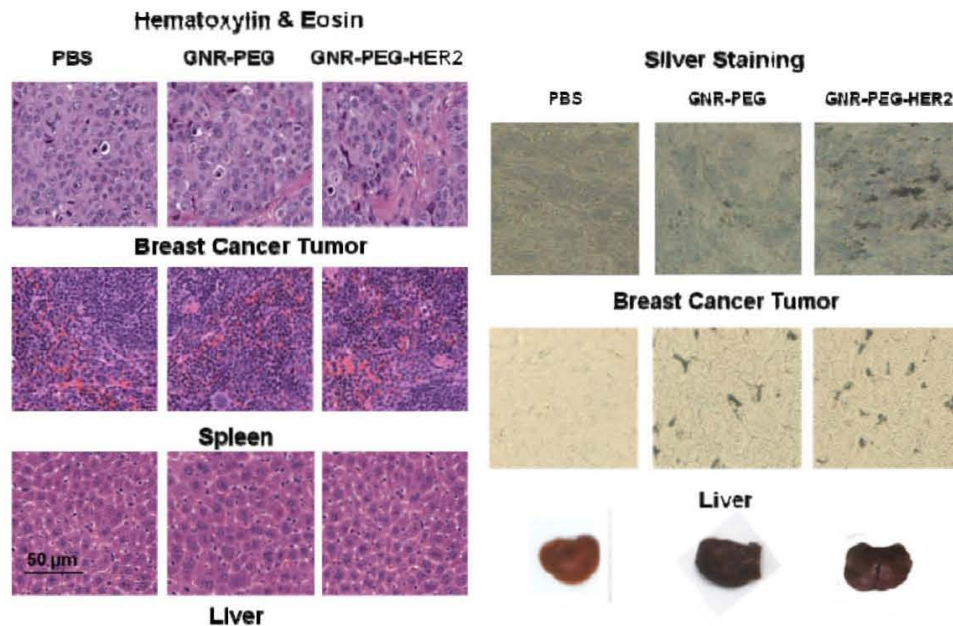


Figure 5. Left: hematoxylin & eosin (tumor, spleen and liver) and Right: silver staining (tumor and liver) of GNR accumulated in mouse tissues following intravenous injection of GNR-PEG or GNR-PEG-HER2 conjugates. Right bottom: slices of liver treated in the same conditions (before paraffin imbedding)

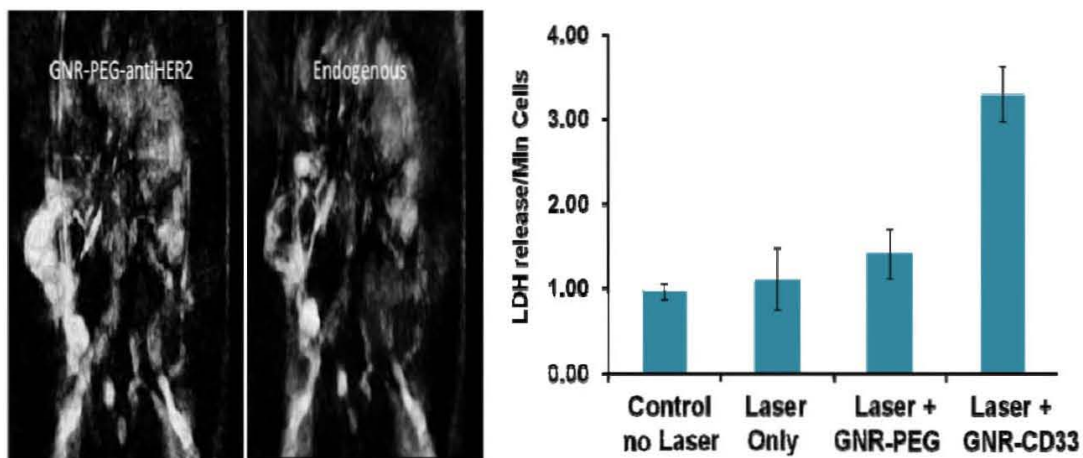


Figure 6. Left: GNR-PEG-mAb images of breast cancer tumor (BT474 tumor with overexpressed HER2 receptor): Mouse body optoacoustic imaging after GNR-PEG-HER2 injection ( $1.4 \times 10^{12}/0.2$  ml, 24 hour), and without injection. Right: pulsed-laser nanothermolysis damage to human acute leukemia cells (HL-60 with overexpressed CD33 receptor) targeted with GNR-CD33 measured as release of LDH from cell to medium

Another application of GNR conjugates is optoacoustic sensing. We have built a single-well NanoLISA prototype (Figure 7). It is designed to be scalable into an 8-channel strip reader which will be compatible with standard 96-well ELISA plates. The device employs forward mode detection of optoacoustic signals generated by the presence of highly absorptive contrast agent present in the sample. Prior to use, the bottom of the wells is coated with a specific antibody targeting the substance of interest (virus, cell, pathogen etc). As the sample is added, elements interacting specifically with the antibody will bind against the bottom of the well: the substance of interest is therefore immobilized. A solution

of biocompatible GNR coated with a specific antibody is then added in order to activate the sample. The presence of immobilized GNR at the bottom of the well indicates the sample contained the targeted substance of interest whose population is therefore proportional to the quantity of contrast agent bound to the bottom of the well. The magnitude of the optoacoustic signal generated by the sample can thus be used to perform quantitative analysis.

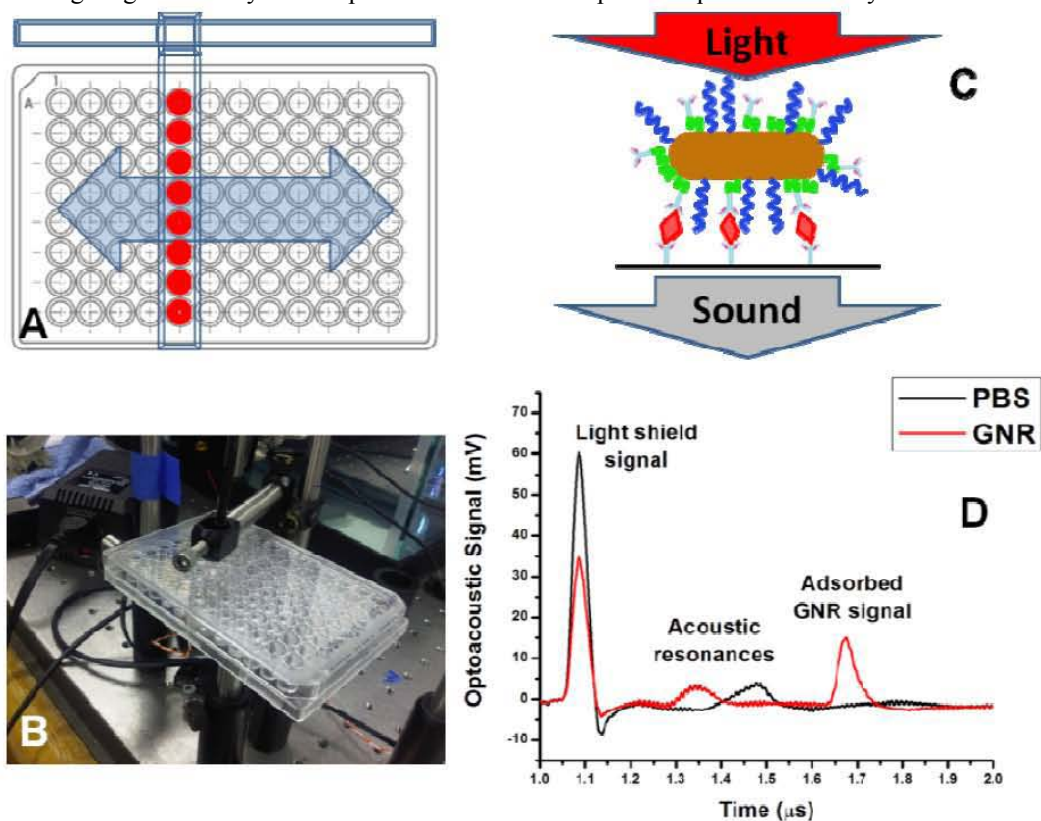


Figure 7. Pictorial representation of the NanoLISA prototype. A) Drawing (top view) of the plate reader investigating one strip at a time, B) picture of current single-well prototype, C) cartoon showing forward-mode conversion of light to sound by conjugated GNR, and D) preliminary result showing forward-mode signal generated by GNR adsorbed onto the bottom of a well.

## CONCLUSION

We have explored and optimized the parameters for improved yield and increased reliability of covalent bonding to conjugate GNRs to the HER2 and CD33 antibody. Covalent attachment of the antibody to GNR and pegylation of these complexes facilitates active targeting by the nanorods for many applications. GNR-PEG-mAb conjugates successfully improve optoacoustic imaging of tumor, increases damage to human acute leukemia cells through pulsed-laser nanothermolysis, and can be used for sensing through the development of NanoLISA.

## ACKNOWLEDGEMENTS

This work was supported by SBIR Grant # R43ES021629 from the National Institute of Environmental Health Sciences and NIH Grant # R44 CA110137-05; R44 CA110137-05S1 and 1R43ES021629-01. We are thankful R. Su and H.P. Brecht for technical assistance during the imaging experiments.

## REFERENCES

- [1] Perez-Juste, J., Pastoria-Santos, I., Liz-Marzan, L. M. and Mulvaney, P., "Gold nanorods: synthesis, characterization, and applications," *Coordination Chemistry Reviews* 249, 1870-1901 (2005).
- [2] Oraevsky, A., [Gold and silver nanoparticles as contrast agents for optoacoustic imaging], Taylor and Francis Group, New York, (2009).
- [3] Khlebstov, N. G. and Dykman, L. A., "Optical properties and biomedical applications of plasmonic nanoparticles," *Journal of Quantitative Spectroscopy and Radiative Transfer* 111, 1-35 (2010).
- [4] Liao, H. and Hafner, J., "Gold nanorod bioconjugates," *Chem. Mater.* 17, 4636-4641 (2005).
- [5] Alkilany, A. M. and Murphy, C. J., "Toxicity and cellular uptake of gold nanoparticles: what we have learned so far?," *J Nanoparticle Research* 12(7), 2313-2333 (2010).
- [6] Tiwari, P. M., Vig, K., Dennis, V. A. and Singh, S. R., "Functionalized gold nanoparticles and their biomedical applications," *Nanomaterials* 1, 31-63 (2011).
- [7] Sau, T. K. and Murphy, C. J., "Seeded High Yield Synthesis of Short Au Nanorods in Aqueous Solution," *Langmuir* 20, 6414-6420 (2004).
- [8] Huang, X., El-Sayed, H. and El-Sayed, M. A., "Applications of gold nanorods for cancer imaging and photothermal therapy," *Methods in Molecular Biology* 624, 343-357 (2010).
- [9] Liao, C. K., Huang, S. W., Wei, C. W. and Li, P. C., "Nanorod-based flow estimation using a high-frame-rate photoacoustic imaging system," *Journal of biomedical optics* 12(6), 064006 (2007).
- [10] Chamberland, D. L., Agarwal, A., Kotov, N., Fowlkes, J. B., Carson, P. L. and Wang, X., "Photoacoustic tomography of joints aided by an Etnarcept-conjugated gold nanoparticle contrast agent -- an ex vivo preliminary rat study," *Nanotechnology* 19, 095101 (2008).
- [11] Niidome, T., Yamagata, M., Okamoto, Y., Akiyama, Y., Takahashi, H. and Kawano, T., "PEG-modified gold nanorods with a stealth character for in vivo applications," *Journal of Controlled Release* 114(3), 343-347 (2006).
- [12] Roberts, M. J., Bentley, M. D. and Harris, J. M., "Chemistry for peptide and protein PEGylation," *Advanced Drug Delivery Reviews* 54, 459-476 (2002).
- [13] Niidome, T., Ohga, A., Watanabe, K., Niidome, Y., Mori, T. and Katayama, Y., "Controlled release of PEG chains from gold nanorods: targeted delivery to tumors," *Bioorganic and Medicinal Chemistry* 18(12), 4453-4458 (2010).
- [14] Rayavarapu, R. G., Petersen, W., Hartsuiker, L., Chin, P., Janssen, H., Leeuwen, F. W. B., Otto, C., Manohar, S. and Leeuwen, T. G., "In vitro toxicity studies of polymer coated gold nanorods," *Nanotechnology* 21, 145101 (2010).
- [15] Urbanska, K., Romanowska-Dixon, B. and Matuszak, Z., "Indocyanine green as a prospective sensitizer for photodynamic therapy of melanomas," *Acta. Biochim. Pol.* 49, 387-391 (2002).
- [16] Lapotko, D., Lukianova, E., Potapnev, M., Aleinikova, O., Oraevsky, A., "Method of laser activated nanothermolysis for elimination of tumor cells," *Cancer Lett.* 239(1), 36-45 (2006).
- [17] Liopo, A. V., Conjusteau, A., Konopleva, M., Andreeff, M. and Oraevsky, A. A., "Photothermal therapy of acute leukemia cells in the near-infrared region using gold nanorods CD-33 conjugates," *Proceedings SPIE* 7897, 789710 (2011).
- [18] Maltzahn, G. v., Park, J. H., Agrawal, A., Bandaru, N. K., Das, S. K., Sailor, M. J. and Bhatia, S. N., "Computationally guided photothermal tumor therapy using long-circulating gold nanorod antennas " *Cancer research* 69(9), 3892-3900 (2009).
- [19] Loo, C., Hirsch, L., Lee, M. H., Chang, E., West, J., Halas, N., Drezek, R., "Gold nanoshell bioconjugates for molecular imaging in living cells," *Opt. Lett.* 30(9), 1012-1014 (2005).
- [20] Huang, X., El-Sayed, I. H., Qian, W., El-Sayed, M. A., "Cancer cell imaging and photothermal therapy in the near-infrared region by using gold nanorods," *J Am Chem Soc* 128(6), 2115-2120 (2006).
- [21] Rayavarapu, R. G., Petersen, W., Ungureanu, C., Post, J. N., Van Leeuwen, T. G. and Manohar, S., "Synthesis and bioconjugation of gold nanoparticles as potential molecular probes for light-based imaging techniques.," *International Journal of Biomedical Imaging* 2007, 29817 (2007).
- [22] Green, H. N., Martyshkin, D. V., Rodenburg, C. M. and Rosenthal, E. L., "Gold nanorod bioconjugates for active tumor targeting and photothermal therapy," *Journal of Nanotechnology* Article ID 631753, (2011).
- [23] Nikoobakht, B. and El-Sayed, M. A., "Preparation and growth mechanism of gold nanorods (NRs) using seed-mediated growth method," *Chemical Materials* 15, 1957-1962 (2003).
- [24] Su, R., Liopo, A. V., Brecht, H. P., Ermilov, S. A. and Oraevsky, A. A., "Gold nanorod distribution in mouse tissues after intravenous injection monitored with optoacoustic tomography," *Proceedings SPIE* 7899, 78994B (2011).

- [25] Eghtedari, M., Liopo, A. V., Copland, J. A., Oraevsky, A. A. and Motamedi, M., "Engineering of Hetero-Functional Gold Nanorods for the in vivo Molecular Targeting of Breast Cancer Cells," *Nano letters* 9(1), 287-291 (2009).
- [26] Chumakova, O. V., Liopo, A., Andreev, V. G., Cicenaite, I., Evers, B. M., Chakrabarty, S., Pappas, T. C. and Esenaliev, R. O., "Composition of PLGA and PEI/DNA nanoparticle improves ultrasound-mediated gene delivery in solid tumor in vivo," *Cancer letters* 261(2), 215-225 (2008).
- [27] Liopo, A., Stewart, M. P., Hudson, J., Tour, J. M. and Pappas, T. C., "Biocompatibility of Native and Functionalized Single-Walled Carbon Nanotubes for Neuronal Interface " *J Nanosci Nanotechnol* 6(5), 1365-1374 (2006).
- [28] Brecht, H. P., Su, R., Fronheiser, M., Ermilov, S. A., Conjusteau, A. and Oraevsky, A. A., "Whole-body three-dimensional optoacoustic tomography system for small animals," *Journal of biomedical optics* 14, 064007 (2009).
- [29] Ermilov, S. A., Khamapirad, T., Conjusteau, A., Leonard, M. H., Lacewell, R., Mehta, K., Miller, T. and Oraevsky, A. A., "Laser optoacoustic imaging system for detection of breast cancer," *Journal of biomedical optics* 14, 024007 (2009).
- [30] Maswadi, S. M., Page, L., Woodward, L., Glickman, R.D., Barsalou, N., "Optoacoustic sensing of ocular bacterial antigen using targeted gold nanorods," *Proceedings SPIE* 6856, 151-158 (2008).
- [31] Conjusteau, A., Maswadi, S. M., Ermilov, S. A., Brecht, H. P., Barsalou, N., Glickman, R. D. and Oraevsky, A. A., "Detection of gold-nanorod targeted pathogens using optical and piezoelectric optoacoustic sensors: comparative study," *Proceedings SPIE* 7177, 71771P (2009).
- [32] Conjusteau, A., Liopo, A. V., Tsyboulski, D., Ermilov, S. A., Elliott, W. R., Barsalou, N., Maswadi, S. M., Glickman, R. D. and Oraevsky, A. A., "Optoacoustic sensor for nanoparticle linked immunosorbent assay (NanoLISA)," *Proceedings SPIE* 7899, 789910 (2011).